Front. Electr. Electron. Eng. China (2006) 2: 146–152
DOI 10.1007/s 11460-006-0006-3

RESEARCH ARTICLE

WANG Shao-yuan, WANG Yao-nan

Image edge detection based on multi-fractal spectrum analysis

Abstract In this paper, an image edge detection method based on multi-fractal spectrum analysis is presented. The coarse grain Hölder exponent of the image pixels is first computed. then, its multi-fractal spectrum is estimated by the kernel estimation method. Finally, the image edge detection is done by means of different multi-fractal spectrum values. Simulation results show that this method is efficient and has better locality compared with the traditional edge detection methods such as the Sobel method.

Keywords Image edge detection, Multi-fractal spectrum, Hölder singular exponent, Kernel estimation

1 Introduction

Multi-fractal, also called multi-resolution fractal or complex fractal [1–3], is a good mathematical tool for depicting singular signal structures, and is always used to describe a singular probability distribution that cannot be depicted by a single fractal indicator parameter only (fractal dimension). Multi-fractal analysis of signals has good performance on both local characteristics and global characteristics, which depicts signals' local characteristics, geometric characteristics and probability distribution (multi-fractal spectrum) describing the signals' global characteristics. Multi-fractal analysis has good performance on both local and global ability. It is a good tool for processing and analyzing images that are irregular and difficult to model. Multi-fractal analysis provides a new way for image edge detection.

Some basic definitions and concepts of multi-fractal spectrum are covered in Sect. 2. In Sect. 3, multi-fractal spectrum estimation based on the kernel estimation method is discussed. Image edge detection algorithm based on multi-fractal spectrum analysis, image edge detection simulation results and analysis are presented in Sect. 4. Sect. 5 concludes this paper.

Translated from *Journal of Hunan University(Natural Sciences)*, 2004, 31(4): 28-33

WANG Shao-yuan(✉), WANG Yao-nan
College of Electrical and Information Engineering, Hunan University, Changsha 410082, China
E-mail: 13873178728@hnmcc.com

2 Multi-fractal analysis basics

Definition 1 Assume $f(x)$ is a function of $f: R \to R$, and

$$\left| f(x) - P(x - x_0) \right| < C \left| x - x_0 \right|^{\alpha} \tag{1}$$

where $\alpha > 0$, P is a polynomial with the order not great than α, and C is a constant greater than 0.
Let:

$$\alpha(x_0) = \sup\{\alpha : f \in C_{x_0}^{\alpha}\} \tag{2}$$

$$\alpha(x) = \sup\left\{\alpha : f \in C_{x}^{\alpha}\right\} \tag{3}$$

We call $\alpha(x_0)$ as the Hölder exponent of function $f(x)$ at the point x_0, and $\alpha(x)$ as the Hölder function of $f(x)$.

From the above definition, we can see that Hölder exponent α is a good description of $f(x)$ with excellent local characteristics.

Definition 2 [1] suppose E_{α} is a point set with Hölder exponent α, and let:

$$f_h(\alpha) = \dim_h(E_{\alpha}) \tag{4}$$

where $\dim_h(E_{\alpha})$ is the Hausdorff dimension of E_{α}. Then we call $f_h(\alpha)$ as the Hausdorff spectrum of E_{α}.

Definition 3 [1] Let $c = (c_n)$ as a capacity sequence defined on $[0,1)$, with values on $[0,1)$. Let μ be a non-atomic reference probability measure. I_n^k is a right semi-open interval on the interval of $[0,1)\times[0,1)$, which

meets $\lim_{n\to\infty}\max_{0\le k\le v_n}\left|I_n^k\right|=0$.

Let $P=\left(\left(I_n^k\right)_{0\le k\le v_n}\right)_{n\ge 1}$ be a partition sequence of $[0,1)\times[0,1)$, v_n be an increasing positive integer sequence. Suppose $I_n(x,y)$ is an interval of I_n^k including (x,y). The coarse grain Hölder exponent is defined as:

$$\alpha_n(x,y)=\frac{\log c_n\left(I_n(x,y)\right)}{\log \mu\left(I_n(x,y)\right)}$$

And its point Hölder exponent is:

$$\alpha(x,y)=\lim_{n\to\infty}\alpha_n(x,y) \tag{5}$$

When the limitation of Eq. (5) exists, let:

$$E_\alpha=\{(x,y),x,y\in[0,1)\times[0,1),\ \alpha(x,y)=\alpha\}$$

Then the Hausdorff singularity spectrum of c related to μ is defined as:

$$f_h(\alpha)=\dim_\mu(E_\alpha) \tag{6}$$

Definition 4 [1] Let $n\in N$, $\varepsilon>0$, $N_n^\varepsilon(\alpha)=\#\{k\in\{0,1,\cdots,v_n-1\},\ \alpha-\varepsilon\le\alpha_n^k\le\alpha+\varepsilon\}$ where $\#\{\cdot\}$ denotes the element number of the set.

Let: $\alpha_n^k=\log c_n\left(I_n^k\right)/\log\mu\left(I_n^k\right)$,

$$f_g^\varepsilon(\alpha)=\limsup_{n\to\infty}\frac{\log N_n^\varepsilon(\alpha)}{\log v_n} \tag{7}$$

Then,

$$\begin{aligned}f_g(\alpha)&=\lim_{\varepsilon\to 0}f_g^\varepsilon(\alpha)\\&=\lim_{\varepsilon\to 0}\lim_{n\to\infty}\frac{\log N_n^\varepsilon(\alpha)}{\log v_n}\end{aligned} \tag{8}$$

We call $f_g^\varepsilon(\alpha)$ and $f_g(\alpha)$ the coarse grain and deviation spectrum of α, respectively.

Furthermore, when I_n^k is a binominal interval ($I_n^k=[k2^{-n},(k+1)2^{-n})\times[k2^{-n},(k+1)2^{-n})$), the reference measure μ is a Lebesgue measure. From Eqs. (7) and (8), we can get:

$$f_g^\varepsilon(\alpha)=\lim_{n\to+\infty}\sup\frac{\log_2 N_n^\varepsilon(\alpha)}{n} \tag{9}$$

$$f_g(\alpha)=\lim_{\varepsilon\to 0}\lim_{n\to+\infty}\sup\frac{\log_2 N_n^\varepsilon(\alpha)}{n} \tag{10}$$

Definition 5 [1] Let

$$M_n(x,y)=\sum_{k=0}^{v_n}\left(c_n\left(I_n^k\right)^x\mu\left(I_n^k\right)^{-y}\right)$$

$$M(x,y)=\lim_{n\to+\infty}\left(\sup\frac{\log M_n(x,y)}{n}\right)$$

$$\Omega=\{(x,y):X(x,y)<0\}$$

where $c_n\left(I_n^k\right)\mu\left(I_n^k\right)\ne 0$, then there exists a concave function τ, such that:

$$\dot\Omega=\left\{(x,y)\in R^2:y<\tau(x-0)\right\}$$

Let τ^* be the Legendre multi-fractal spectrum of τ, then the Legendre transform of τ can be defined as:

$$\begin{aligned}f_l(\alpha)&=\tau^*(\alpha)\\&=\inf_q\left[q\alpha-\tau(q)\right]\end{aligned} \tag{11}$$

We call $f_l(\alpha)$ the Legendre spectrum of α. If the intervals' sizes ($\left|I_n^k\right|$) are all the same and μ is a Lebesgue measure, τ can be defined as:

$$\tau(q)=\lim_{n\to+\infty}\sup\frac{\log\sum_k\mu\left(I_n^k\right)^q}{-n}\qquad\left(I_n^k\right)\ne 0$$

From Eqs. (6), (10) and (11), we can see that f_h is a Hausdorff dimension for a given point set with Hölder exponent α, and it is a geometry description of singular point distribution; f_g is the probability finding a point with coarse grain Hölder exponent $\alpha_n(x,y)$, and it is a probability description of singular point distribution; while f_l is a Legendre transform of the Renyi exponent $\tau(q)$ of qth moment of measure μ. In some special case $f_l=f_g=f_h$ [4-5], but $f_l\ge f_g\ge f_h$ [6–9] generally holds.

Definition 6 Suppose G is a digital image defined on $[0,1]\times[0,1]$, and $P=\{p_n\}$, $p_n=\left(\left(I_k^n\right),\ 0\le k\le 2^n-1\right)$ is a partition sequence on $[0,1]\times[0,1]$. Let $\left(x_k^n,y_k^n\right)$ be a certain point on I_k^n. $L\left(I_k^n\right)$ is the gray level sum of I_k^n, $L(x,y)$ is the gray level at the point (x,y) of G, and Ω is a certain region of G. We can define the following three capacity measures of G:

Sum capacity:

$$c^s(\Omega)=\sum_{(x,y)\in\Omega}L(x,y)$$

Max capacity:

$$\begin{aligned}&c_n^m(\Omega)=\max L\left(I_{n+p_n}^k\right)\\&\forall I_{n+p_n}^k,\left(x_{n+p_n}^k,y_{n+p_n}^k\right)\in\Omega\\&c^M(\Omega)=\max_{(x,y)\in\Omega}L(x,y)\end{aligned}$$

Isometric capacity:

$$\begin{aligned}&c_n^i(\Omega)=\max_l\ \#\left\{k:(x,y)\in\Omega,\ L\left(I_{n+p_n}^k\right)=l\right\}\\&c^I(\Omega)=\max_l\ \#\{(x,y):(x,y)\in\Omega,L(x,y)=l\}\end{aligned}$$

From the definition of the three capacity measures, we can see that $c^s(\Omega)$ relies on both the gray and gray distribution, $c_n^m(\Omega)$ and $c^M(\Omega)$ are only on the gray

levels, while $c_n^i(\Omega)$ and $c^I(\Omega)$ are only on gray distribution. Furthermore, $\left(c_n^m, c^M\right)$ and $\left(c_n^i, c^I\right)$ can be used to represent the image orthogonal information, and also have good performance of anti-noise. Figure 1(a), 1(b) is the Hölder exponent of $c^s(\Omega)$ and $c^M(\Omega)$ capacity of the original Lenna image shown in Fig. 2(a).

(a)

(b)

Fig. 1 Hölder exponents of different capacities.(a) Hölder exponent of $c^s(\Omega)$; (b) Hölder exponent of $c^M(\Omega)$

3 Multi-fractal spectrum estimation

From the Eqs. (6), (10) and (11), we can see that the computation of $f_l(\alpha)$ is the simplest. But $f_l(\alpha)$ is a concave function, some of its detailed spectrum information is also left out. $f_h(\alpha)$ is defined as the Hausdorff dimension of sets of points having the same Hölder exponent α, so it is the most computationally complex. While the computation of $f_g(\alpha)$ is relatively simple compared with that of $f_h(\alpha)$, it can retain the most detailed spectrum information compared with that of $f_l(\alpha)$. This section focuses on the estimation of $f_g(\alpha)$.

3.1 Histogram estimation method

The histogram estimation method is the simplest and most commonly used density estimation method. Estimation of $f_g(\alpha)$ using the histogram method is as follows:

1) Choose a proper capacity sequence $\{c_n\}$ and a reference measure μ.

2) For each resolution n, compute all coarse grain Hölder exponents α_n^k ($\alpha_n^k = \log c_n\left(I_n^k\right) \Big/ \log \mu\left(I_n^k\right)$).

3) Compute the maximum and minimum of α_n^k.

$$\alpha_n^{\max} = \max_k \left\{\alpha_n^k\right\}$$

$$\alpha_n^{\min} = \min_k \left\{\alpha_n^k\right\}$$

4) Divide $[\alpha_n^{\min}, \alpha_n^{\max}]$ into N boxes B_N^i ($\left|B_N^i\right| = \left|[\alpha_n^{\min}, \alpha_n^{\max}]\right| / N$).

5) Compute the number of intervals I_n^k whose α_n^k falls in the ith box.

$$N_n^i = \#\left\{I_n^k : \alpha_n^k \in B_N^i,\ i = 1, 2, \cdots, N\right\}.$$

6) Estimate $f_g(\alpha)$ by a linear regression on $\left(\log N_n^i, \log n\right)$.

The histogram method can achieve satisfactory results for strictly stationary processes. But for some non-stationary and multiplicative processes, especially when $f_g(\alpha)$ is not a concave function, some important detailed information may be left out. Another problem for the estimation of f_g using the histogram method is that the limitation relationship between f_g and ε is not concerned when the box number is selected on α. Thus, estimation of f_g using the histogram method cannot always achieve good results.

3.2 Kernel estimation method

Nonparametric density estimation started from Chen [10] and Devroye's [11] work. Based on histogram density estimation, they proposed a kind of effective density estimation method called kernel density estimation. Since kernel density estimation is a nonparametric density estimation method, we can use it to estimate f_g. The precondition of kernel estimation is that f_g must be the density function of α. But from Eq. (10), we can see that f_g is not the density function of α. So kernel estimation method cannot be directly used on f_g. In order to estimate f_g using kernel density estimation, f_g must be redefined as the form of density function of α.

Let P_n be an interval partition sequence on $[0, 1)\times[0, 1)$,

$$P_n = \left\{I_n^k,\ 0 \le k \le 2^n - 1\right\}$$

$$I_n^k = [k2^{-n}, (k+1)2^{-n}) \times [k2^{-n},\ (k+1)2^{-n})$$

For now, we can rewrite $N_n^{\varepsilon}(\alpha)$ as the following convolution form:

$$\begin{aligned} N_n^{\varepsilon}(\alpha) &= \sum_{k=0}^{2^n-1} L_{[-\varepsilon,+\varepsilon]}\left(\alpha-\alpha_n^k\right) \\ &= 2^{n+1}\varepsilon\left(p_n \times L_{[-\varepsilon,+\varepsilon]}\right)(\alpha) \end{aligned} \tag{12}$$

where $B(\alpha,\varepsilon)$ is a ball centered on α and its radius is ε. $L_{[-\varepsilon,+\varepsilon]}(x)$ is an indicator function meeting Eq. (13). It can be substituted by any compactly supported kernel K as $\int_D K=1$ (D is the support of K), and $p_n(\alpha)$ is the empirical probability density function of coarse grain Hölder exponent $\left(\alpha_k^n\right)_k$.

$$\int_{-\varepsilon}^{+\varepsilon} L_{[-\varepsilon,+\varepsilon]}(x)\,\mathrm{d}x=1,\quad \forall x\in[-\varepsilon,+\varepsilon] \tag{13}$$

Then

$$\begin{aligned} p_n(\alpha) &= 2^{-n}\sum_{k=0}^{2^n-1}\delta\left(\alpha-\alpha_n^k\right) \\ \delta(x) &= \begin{cases} 1, & x=0 \\ 0, & \text{others} \end{cases} \end{aligned} \tag{14}$$

Let $K_{\varepsilon}(\alpha)=(1/2\varepsilon)K\left(\frac{\alpha}{\varepsilon}\right)$ be an admissible compactly supported kernel function, then

$$p_n^{\varepsilon}(\alpha)=2\varepsilon\left(p_n * K_{\varepsilon}\right)(\alpha)=\frac{N_n^{\varepsilon}(\alpha)}{2^n} \tag{15}$$

From Eq. (10), (12) and (15), we can get

$$\begin{aligned} f_g(\alpha) &= \lim_{\varepsilon\to 0}\limsup_{n\to\infty}\frac{\log_2\left(2^{n+1}\varepsilon\left(p_n * K\varepsilon\right)(\alpha)\right)}{n} \\ &= 1+\lim_{\varepsilon\to 0}\limsup_{n\to\infty}\left(\frac{1}{n}\log_2 p_n^{\varepsilon}(\alpha)\right) \end{aligned} \tag{16}$$

In Eq. (16), the estimation of $f_g(\alpha)$ must consider the relationship of ε and α, and also of ε and n. At the same time the stability of estimation results at each resolution of n must also be concerned [10–12]. This is the most important for the estimation of $f_g(\alpha)$ by the kernel estimation method. In fact, it is very difficult to determine the relationship of all parameters. In order to overcome these difficulties, we must redefine Eq. (14).

Suppose I is the interval of size η ($|I|=\eta$), and its coarse grain Hölder exponent is $\alpha_\eta(I)$ ($\alpha_\eta(I)=\log\mu(I)/\log\eta$). Let $E_\eta(\alpha)$ be the reunion of all intervals of the same size η, whose coarse grain Hölder exponent equals a given Hölder exponent value α.

$$E_\eta(\alpha)=\cup\left\{I\in[0,1),|I|=\eta,\ \alpha_\eta(I)=\alpha\right\}$$

Let p_η be a Lebesgue measure, then

$$p_\eta=\left|E_\eta(\alpha)\right| \tag{17}$$

and

$$p_\eta^{\varepsilon}(\alpha)=\int_{\alpha-\varepsilon}^{\alpha+\varepsilon} p_\eta(\beta)\mathrm{d}\beta=2\varepsilon\left(p_\eta L_{[-\varepsilon,+\varepsilon]}\right)(\alpha) \tag{18}$$

From Eq. (17), we can get

$$f_g(\alpha)=1-\lim_{\varepsilon\to 0}\lim_{\eta\to 0}\inf\left(\frac{\log p_\eta^{\varepsilon}(\alpha)}{\log\eta}\right) \tag{19}$$

Let

$$\begin{cases} \alpha_\eta^-(x)=\inf\left\{\alpha_\eta(I),\ x\in I,\ |I|=\eta\right\} \\ \alpha_\eta^+(x)=\sup\left\{\alpha_\eta(I),\ x\in I,\ |I|=\eta\right\} \\ g_\eta^{\varepsilon}(x,\alpha)=\dfrac{1}{2\varepsilon}\left(\min\left\{\alpha+\varepsilon,\alpha_\eta^+(x)\right\}-\max\left\{\alpha-\varepsilon,\alpha_\eta^-(x)\right\}\right) \end{cases} \tag{20}$$

From Eq. (20), we can get

$$g_\eta^{\varepsilon}(x,\alpha)=\frac{1}{2\varepsilon}\begin{cases} \alpha_\eta^+(x)-\alpha_\eta^-(x), & \alpha-\varepsilon\le\alpha_\eta^-(x)\le\alpha_\eta^+(x)\le\alpha+\varepsilon \\ \alpha_\eta^+(x)-\alpha+\varepsilon, & \alpha_\eta^-(x)\le\alpha-\varepsilon\le\alpha_\eta^+(x)\le\alpha+\varepsilon \\ \alpha+\varepsilon-\alpha_\eta^-(x), & \alpha-\varepsilon\le\alpha_\eta^-(x)\le\alpha+\varepsilon\le\alpha_\eta^+(x) \\ 2\varepsilon, & \alpha_\eta^-(x)\le\alpha-\varepsilon\le\alpha+\varepsilon\le\alpha_\eta^+(x) \end{cases} \tag{21}$$

and

$$g_\eta^{\varepsilon}(x,\alpha)=\frac{1}{2\varepsilon}\left|[\alpha-\varepsilon,\alpha+\varepsilon]\cap\left[\alpha_\eta^-(x),\alpha_\eta^+(x)\right]\right| \tag{22}$$

Performing integral operation on the both sides of Eq. (22), we can get:

$$\begin{aligned} &2\varepsilon\int_{D(\mu)} g_\eta^{\varepsilon}(x,\alpha)\mathrm{d}x \\ &\quad=2\varepsilon\int_{D(\mu)}\frac{1}{2\varepsilon}\left(\int_{\alpha_\eta^-(x)}^{\alpha_\eta^+(x)} L_{[-1,1]}\left(\frac{\beta-\alpha}{\varepsilon}\right)\mathrm{d}\beta\right)\mathrm{d}x \\ &\quad=\int_{-\infty}^{+\infty} L_{[\alpha-\varepsilon,\alpha+\alpha]}(\beta)\left(\int_{D(\mu)} L_{[\alpha_\eta^-(x),\alpha_\eta^-(x)]}(\beta)\,\mathrm{d}x\right)\mathrm{d}\beta \end{aligned} \tag{23}$$

Since

$$\beta\in[\alpha_\eta^-(x),\alpha_\eta^+(x)]\Leftrightarrow\exists I,\ \alpha_\eta(I)=\beta:\ x\in I\Leftrightarrow x\in E_\eta(\beta)$$

then

$$L_{[\alpha_\eta^-(x),\alpha_\eta^+(x)]}=L_{E_\eta(\beta)},\forall(x,\beta)$$

$$\int_{D(\mu)} L_{[\alpha_\eta^-(x),\alpha_\eta^+(x)]}(\beta)\,\mathrm{d}x=\left|E_\eta(\beta)\right|=p_\eta(\beta)$$

From Eq. (23), we can get

$$2\varepsilon\int_{D(\mu)} g_\eta^{\varepsilon}(x,\alpha)\mathrm{d}x=\int_{\alpha-\varepsilon}^{\alpha+\varepsilon} p_\eta(\beta)\mathrm{d}\beta=p_\eta^{\varepsilon}(\alpha) \tag{24}$$

where $D(\mu)$ is the support of μ.

When the kernel function K_ε is introduced in Eq. (22), then

$$g_\eta^{K_\varepsilon}(x,\alpha)=\frac{1}{2\varepsilon}\int_{\alpha_\eta^-(x)}^{\alpha_\eta^+(x)} K\left(\frac{\beta-\alpha}{\varepsilon}\right)\mathrm{d}\beta \tag{25}$$

So Eq. (24) can be represented in the following form:

$$p_\eta^\varepsilon(\alpha)=2\varepsilon\int_{D(\mu)} g_\eta^{K_\varepsilon}(x,\alpha)\mathrm{d}x = 2\varepsilon\left(p_\eta\, K_\varepsilon\right)(\alpha) \tag{26}$$

Furthermore, when $K=L_{[-1,+1]}$

$$g_\eta^{K_\varepsilon}(x,\alpha)=\frac{1}{2\varepsilon}\left|[\alpha-\varepsilon,\alpha+\varepsilon]\cap\left[\alpha_\eta^-(x),\alpha_\eta^+(x)\right]\right| \tag{27}$$

$$\hat{p}_\eta(\alpha)=2\varepsilon\, g_\eta^{K_\varepsilon}(x,\alpha) =\left|[\alpha-\varepsilon,\alpha+\varepsilon]\cap\left[\alpha_\eta^-(x),\alpha_\eta^+(x)\right]\right| \tag{28}$$

$$\hat{p}_\eta^\varepsilon(\alpha)=2\varepsilon\left(\hat{p}_\eta\times L_{[-\varepsilon,+\varepsilon]}\right)(\alpha)$$

$$\hat{f}_{g,\eta}^\varepsilon(\alpha)=1-\frac{\log\hat{p}_\eta^\varepsilon(\alpha)}{\log\eta} \tag{29}$$

In Eq.(29), $\hat{f}_{g,\eta}^\varepsilon(\alpha)$ is the estimated value of the multi-fractal spectrum $f_g(\alpha)$.

4 Image edge detection

4.1 Edge detection algorithm by multi-fractal spectrum

According to the multi-fractal spectrum, image pixels are divided into two kinds: smooth edge point ($f_g(\alpha)=1.0$) and *t*-singular edge point ($f_g(\alpha)=t$, $1.0<t<2.0$).

Smooth edge points and *t*-singular points constitute the edge of the image to be detected.

Now, we generalize the multi-fractal spectrum edge, and detection algorithm in the following steps:

Step 1: Choose a certain capacity sequence $\{c_n\}$ and a reference measure μ;

Step 2: Compute image pixels' coarse grain exponent $\alpha_\eta(i,j)$ on $\{c_n\}$ and μ;

$$\alpha_\eta(i,j)=\frac{\log c\left(I_\eta(i,j)\right)}{\log\mu\left(I_\eta(i,j)\right)}a$$

Step 3: Compute the estimated multi-fractal spectrum value $\hat{f}_{g,\eta}^\varepsilon(\alpha)$ of $f_g(\alpha)$ about $\alpha_\eta(i,j)$;

$$\hat{p}_\eta(\alpha)=2\varepsilon g_\eta^{K_\varepsilon}(i,j,\alpha) =\left|[\alpha-\varepsilon,\alpha+\varepsilon]\cap\left[\alpha_\eta^-(i,j),\alpha_\eta^+(i,j)\right]\right|$$

$$\alpha_\eta^-(i,j)=\inf\left\{\alpha_\eta(I),\ \ i,j\in I,|I|=\eta\right\}$$

$$\alpha_\eta^+(i,j)=\sup\left\{\alpha_\eta(I),\ \ i,j\in I,|I|=\eta\right\}$$

$$\hat{p}_\eta^\varepsilon(\alpha)=2\varepsilon\left(\hat{p}_\eta\times L_{[-\varepsilon,+\varepsilon]}\right)(\alpha)$$

$$\hat{f}_{g,\eta}^\varepsilon(\alpha)=1-\frac{\log\hat{p}_\eta^\varepsilon(\alpha)}{\log\eta}$$

Step 4: Detect image smooth edge points $E_{1.0}$;

$$E_{1.0}=E\left\{(i,j):\hat{f}_{g,\eta}^\varepsilon(\alpha)=1.0\right\}$$

Step 5: Detect all singular edge points E_t ($1.0<\hat{f}_{g,\eta}^\varepsilon(\alpha)\le t$) for a given multi-fractal spectrum threshold t, multi-fractal spectrum of singular edge points are always located on the range of $1.1\le f_g(\alpha)\le 1.5$ [13-14]);

$$E_t=E\left\{(i,j):1.0<\hat{f}_{g,\eta}^\varepsilon\le t\right\}$$

Step 6: Combine image smooth edge $E_{1.0}$ and singular edge E_t ($E_{\text{edge}}=E_{1.0}\cup E_t$)

4.2 Simulation results and analysis

Our simulation test uses the $c^I(\Omega)$ as the capacity measure and the Lebesgue as reference measure μ. The interval size is $\eta=0.003\,906$, and the small deviation value is $\varepsilon=0.007\,25$ and the kernel function is $K=L_{[-1,+1]}$. Fig.2 shows the edge detection results of the original Lenna of size 512 × 512 pixels using multi-fractal spectrum analysis, where Fig. 2(a) is the original image of Lenna, and Fig.2(b) is the Hölder exponent of the original image. Fig.2(c) is a multi-fractal spectrum of Fig. 2(a) while Fig.2(d) is the smooth edge detection result of Fig. 2(a) with $f_g(\alpha)=1.0$. Fig. 2(e), and Fig.2(f) are the edge detection results of the original image with $1.0\le f_g(\alpha)\le 1.1$ and $1.0\le f_g(\alpha)\le 1.2$. Fig. 3 is the Sobel edge detection result of Fig. 2(a), whose threshold value equals 10. From Figs. 2-3, we can see that a finer edge can be detected than the Sobel method when the multi-fractal spectrum value $f_g(\alpha)$ is properly chosen.

Fig. 3 Sobel edge detection result (*TH*=10)

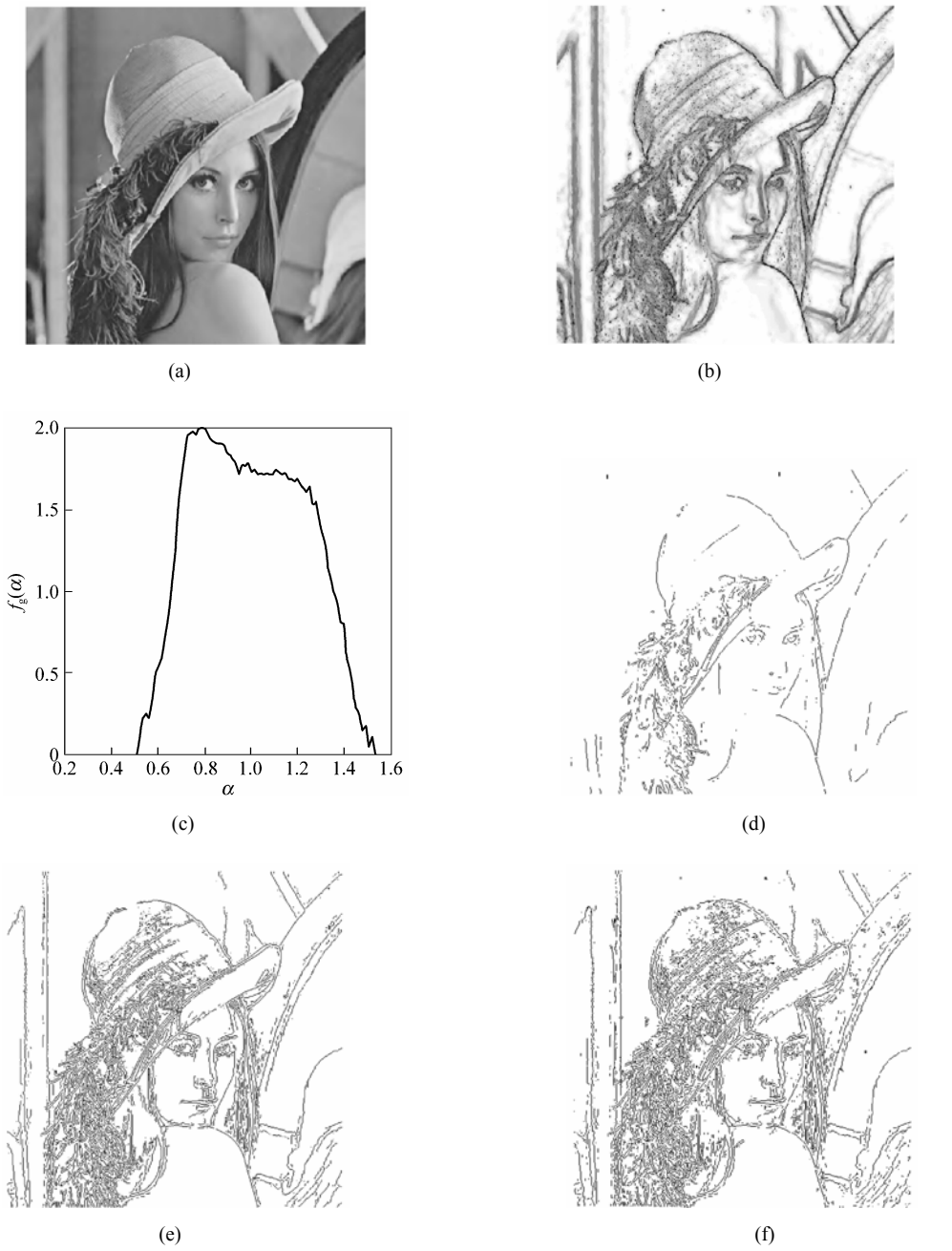

Fig. 2 Multi-fractal spectrum edge detection. (a) The original image Lenna 512×512 ; (b) The Hölder exponent of $c^l(\Omega)$; (c) The estimated spectrum of $f_g(\alpha)$; (d) The edge detection result with $\hat{f}^{\varepsilon}_{g,\eta}=1.0$; (e) The edge detection result($1.0\le\hat{f}^{\varepsilon}_{g,\eta}\le1.1$); (f) The edge detection result ($1.0\le\hat{f}^{\varepsilon}_{g,\eta}\le1.2$)

5 Conclusions

Multi-fractal analysis is a good mathematic tool for depicting singular signal structure. It is always used to describe a singular probability distribution, which cannot be depicted by a single fractal indicator parameter only. Multi-fractal analysis of signals has good performance on both local characteristics and global characteristics. In this paper, a novel image edge detection using multi-fractal spectrum is given in which the Hölder exponent $\alpha(i,j)$ of the given image is firstly computed. Then, the multi-fractal spectrum $f(\alpha)$ of $\alpha(i,j)$ is estimated. Finally, according to the value of $f(\alpha)$, the image edge

points are detected. As the $f(\alpha)$ value of the edge points is always between 1.0 and 1.5, the larger $f(\alpha)$ value providing the finer edge can be detected. Simulation results show that edge detection by multi-fractal spectrum analysis method has better locality than traditional ones making it a good alternative for image edge detection.

Acknowledgements Supported by National Natural Science Foundation of China(Grant No.60375001)

References

1. Riedi R., Introduction to multi-fractals, Rice University, 1997
2. Zhang J. H., Fractal, Tsinghua University Publishing House, 1995
3. Xie H., Mathematic foundation and methods in fractal applications, Science publishing House, 1998
4. Riedi R., An improved multi-fractal formalism and self-similar measures, Pac. J. Math., 1995, 189: 462–490
5. Holley R., Waymire E., Multi-fractal dimensions and scaling exponents for strongly bounded random cascade, Ann. Appl. Probab., 1992, 2(4): 819–845
6. Brown G., Michon G., On the multi-fractal analysis of measure, J. Stat. Phys., 1992, 66: 775–790
7. Lévy Véhe J. L Vojak R., Multi-fractal analysis of Choquet capacities: preliminary result, Adv. Appl. Math., 1998, 20(1): 1–43
8. Mandelbrot B. B., Multi-fractal measures, Chaos and Fractals: New frontiers in Science, 1989, 40(9): 5284–5294
9. Cates M. E., Deutsch J. M., Spatial correlation in multi-fractal, Phys. Rev. A, 1987, 35(11): 4907–4910
10. Chen X., None parametric estimation, Shanghai Science and Technology Publishing House, 1989
11. Devroye L., None Parametric Density Estimation, New York, 1984
12. Lepskii O., Mammem E., Optimal spatial adaptation to inhomogeneous smooth: an approach based on kernel estimates with variable bandwidth selector, Ann. Stat., 1997, 25(3): 929–947
13. Arbeiter M., Patzschke N., Random self-similar multi-fractal, Pac. J. Math., 1996, 181: 5–42
14. Falconer K. J., The multi-fractal spectrum of statistically self-similar measures, J. Theor. Probab., 1994, 7(3): 123–130